EARLY RESULTS FROM NOAA-21 (JPSS-2) VIIRS ON-ORBIT CALIBRATION

X. Xiong[1], A. Angal[2], J. Sun[2], N. Lei[2], K. Twedt[2], and K. Chiang[2]

[1]Sciences and Exploration Directorate, NASA/GSFC, Greenbelt, MD 20771, USA
[2]Science Systems and Applications, Inc., Lanham, MD 20706, USA

ABSTRACT

Launched on November 10, 2022, the NOAA-21 (N-21) VIIRS has successfully completed its initial post-launch testing (PLT) and intensive calibration and validation (ICV) activities. It is now operated in its nominal configuration and characterized using measurements from its on-board calibrators (OBC) and lunar observations. In this paper, we provide a brief description of N-21 VIIRS on-orbit operation and calibration activities and present results derived from its early mission performance assessments, including examples of its OBC performance, spectral band responses, as well as detector signal to noise characteristics. As shown in this paper, the overall performance of N-21 VIIRS is better than that of its predecessor currently operated on the S-NPP and comparable to the one onboard the N-20, with an exception of relatively large changes in its SWIR band responses.

Index Terms **-** NOAA-21, VIIRS, on-orbit calibration

1. INTRODUCTION

The VIIRS is one of the key instruments on-board the JPSS-2 satellite, also referred to as the N-21 following its launch on November 10, 2022, currently operated in tandem with S-NPP and NOAA-20 (N-20) satellites launched on October 28, 2011 and November 18, 2017, respectively. Near-identical VIIRS instruments will also be onboard the JPSS-3 and JPSS-4 satellites that are scheduled to launch in 2027 and 2033, respectively [1]. The VIIRS collects data in 22 spectral bands, including M1-M16 (moderate resolution bands), I1-I5 (imaging bands), and DNB (day and night band). Among them, M1-M11 and I1-I3, with wavelengths from 0.41 to 2.2 μm, are the reflective solar bands (RSB) and bands M12-M16 and I4-I5, covering wavelengths from 3.7 to 12 μm, are the thermal emissive bands (TEB). Seven of the M bands (M1-M5, M7, and M13) are the dual gain bands that can make observations at either high- or low-gain. The DNB can collect data at three different gain stages and thus covers an extremely large dynamic range.

The calibrated VIIRS observations or its sensor data records (SDR) include scene radiances, reflectances, and brightness temperatures and serve as input for producing various environmental data records (EDR). The VIIRS EDR support a broad range of operational applications and scientific studies and further extend many of the long-term data records generated from MODIS observations [2-6]. As expected, the EDR quality depends strongly on the quality of its SDR and thus the sensor on-orbit performance in terms of its calibration accuracy and stability. This paper provides a brief description of N-21 VIIRS early mission operation and calibration activities, including the calibration maneuvers, and presents its on-orbit performance using examples derived from its OBC measurements and lunar observations. Early results show that the N-21 VIIRS on-orbit performance meets its overall design requirements and is generally better than its predecessor currently operated on S-NPP and comparable to the one on N-20 [7-9]. An exception is that the N-21 VIIRS has experienced relatively large change in its SWIR band responses. Also discussed in this paper are future calibration activities and improvement strategies as more calibration data become available.

2. ON-ORBIT CALIBRATION

The VIIRS on-orbit calibration is performed primarily using measurements made from a set of OBC that include a solar diffuser (SD), a solar diffuser stability monitor (SDSM), and a blackbody (BB). The SD provides on-orbit calibration reference for the RSB and the BB calibrates the TEB. In addition, regularly scheduled lunar observations made through the instrument's space view (SV) port provide an independent stability monitoring for the RSB and calibration adjustments on an as needed basis [7]. Illustrated in Fig. 1 are the VIIRS instrument, its rotating telescope assembly (RTA), and on-board calibrators.

Shortly after launch, the N-21 experienced an anomaly with its Ka-transmitter on December 16, 2022. Following a series of comprehensive diagnostic testing, a decision was made to switch to the secondary Ka-transmitter. This anomaly led to a large data gap of 48 days. To date, the N-21 VIIRS has completed all the planned PLT and ICV activities, including various calibration maneuvers and mid-mission outgassing (MMOG). It is now operated in a nominal configuration with BB temperature set at 292.5 K and cold focal plane assembly (CFPA) temperature set at 80 K (changed from initial setting of 82 K). The VIIRS SD views the Sun through an attenuation screen and calibrates

the RSB every orbit. Its on-orbit degradation is tracked regularly by the SDSM with 8 filtered detectors (D1 to D8) covering wavelengths from 0.41 to 0.93 μm. In general, the SDSM operation is performed every orbit at mission beginning and gradually reduced to daily and weekly intervals. As of May 20, 2023, the N-21 has performed 3 scheduled lunar observations.

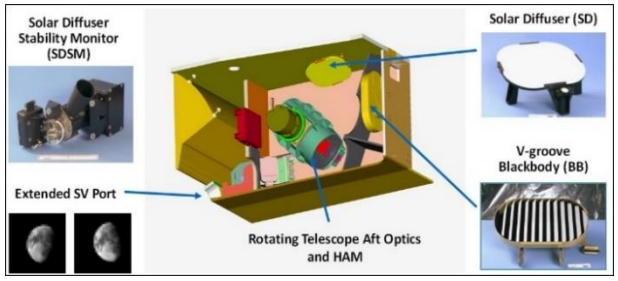

Fig. 1 VIIRS instrument, its rotating telescope assembly (RTA), and on-board calibrators (OBC).

In addition to roll maneuvers regularly performed for the lunar observations, the spacecraft also performed the yaw and pitch maneuvers at the mission beginning, allowing VIIRS to collect special data to help validate, derive, and improve several key calibration parameters, such as TEB response versus scan-angle (RVS), the SD and SDSM screen transmission functions, and the DNB offset tables.

3. INSTRUMENT PERFORMANCE

Due to frequent solar exposure, the VIIRS SD bidirectional reflectance distribution function (BRDF) degrades on-orbit. Fig. 2 shows the N-21 VIIRS SD on-orbit degradation since launch at wavelengths of its detectors 1-8 (D1: 0.41 μm, D2: 0.44 μm, D3: 0.49 μm, D4: 0.56 μm, D5: 0.67 μm, D6: 0.75 μm, D7: 0.86 μm, D8: 0.93 μm). The large data gap (days 37-85) was due to the spacecraft Ka-transmitter anomaly occurred shortly after launch. The overall SD degradation trends of N-21 are very similar to that of S-NPP and N-21, with large changes at short wavelengths.

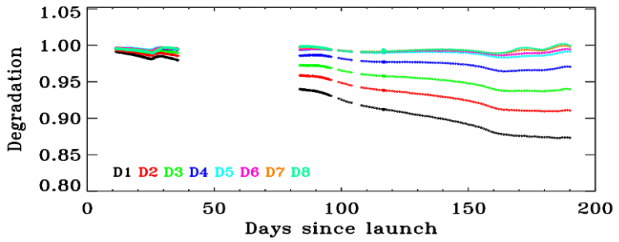

Fig. 2 SD on-orbit degradation at different detector wavlengths (D1-D8: 0.41-0.93 μm).

The on-board BB is the calibration source for the TEB and is nominally controlled at 292.5 K except during its warm-up/cool-down (WUCD) and spacecraft or instrument safe hold events. Fig. 3 illustrates N-21 VIIRS BB performance, in terms of its (a) short-term stability and (b) spatial uniformity. The BB short-term stability is demonstrated by the scan-by-scan temperatures averaged over its six thermistors and its spatial uniformity by their standard deviations. As shown in Fig. 3, the BB performance in the nighttime orbits is more stable and uniform than in the daytime orbits. During part of the daytime orbits, the N-21 VIIRS BB spatial uniformity fails to meet the specified requirements of 30 mK. Meanwhile, both S-NPP and N-20 VIIRS BB show good uniformity that meets the specified requirements. The N-21 VIIRS performed its first BB WUCD on March 10, 2023, which enabled a more comprehensive assessment of TEB on-orbit performance.

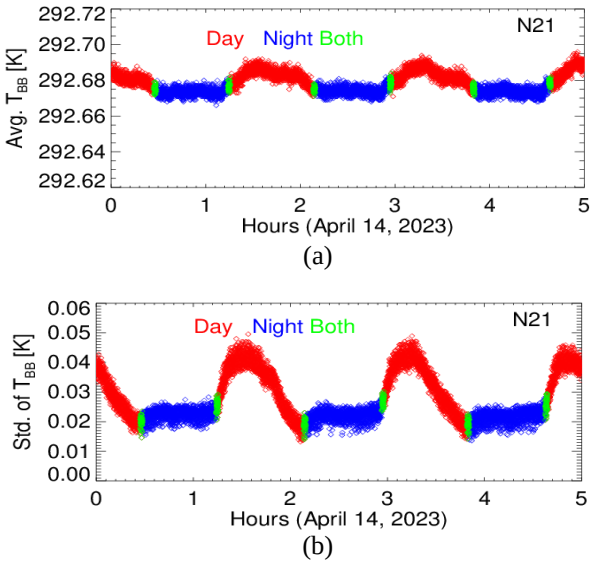

Fig. 3 BB temperature (a) short-term stability and (b) spatial uniformity. The nightime/daytime data are shown in blue/red color and data with both daytime and nighttime are in green color.

Presented in Fig. 4 are on-orbit changes in spectral band responses (or normalized gains) of N-21 VIIRS for (a) bands with wavelengths less than 0.5 μm (M1-M3); (b) bands within 0.5-1.0 μm (I1, I2, and M4-M7); (c) SWIR bands (I3, M8-M11) with wavelengths in 1.0-2.3 μm, and (d) TEB (I4, I5, M12-M16) with wavelengths above 3.5 μm. The detector gains are equivalent to 1/F-factors with F-factors (or the calibration scaling factors) derived using sensor responses to the calibration source or target, such as on-board SD for the RSB and BB for the TEB. Results shown in Fig. 4 are averaged over all detectors within a band for HAM side-A and high gain (HG) for the dual gain bands. For N-21, the VIS and NIR data became available shortly after the instrument switched to its science mode on Nov 20, 2022. Except for the orbits at very beginning, the N-21 VIS and NIR responses have been stable. This performance is very similar to that of N-20 VIIRS and better

than that of S-NPP. As mentioned earlier, the large data gap in the spectral band responses was due to the spacecraft Ka-transmitter anomaly. .

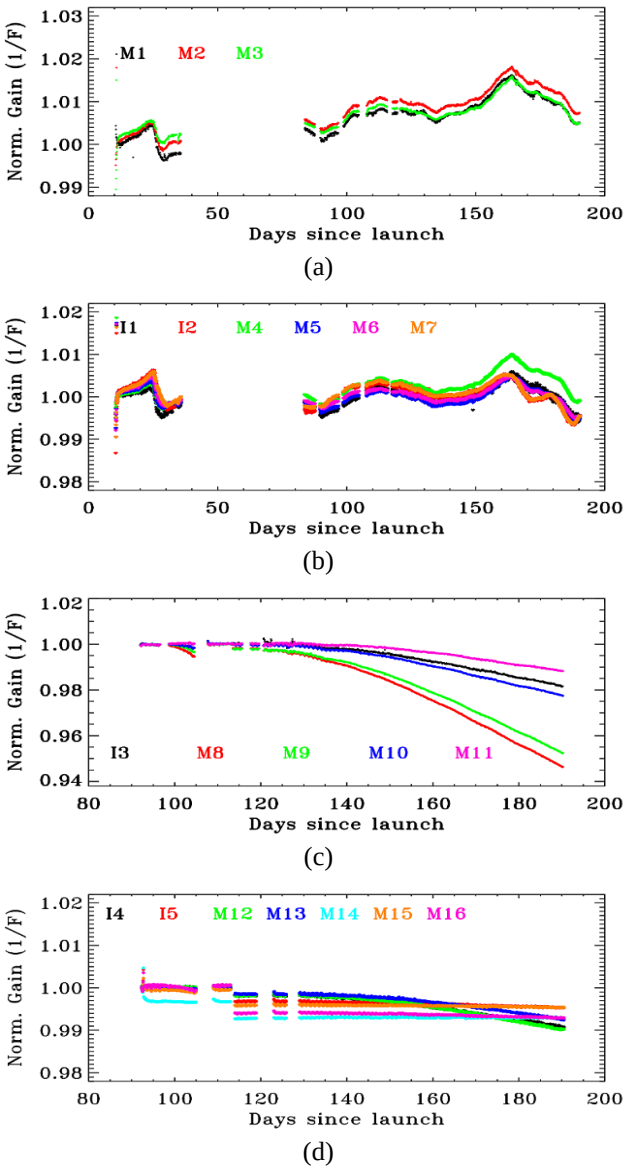

Fig. 4 Spectral band reponses (normalized gains or 1/F-factors) deived from SD/SDSM calibration data: (a) M1-M3, (b) I1, I2, and M4-M7, (c) I3, M8-M11, and (d) I4, I5, and M12-M16 (see text for details).

The SWIR bands and TEB are located on the CFPA. Their on-orbit responses were not fully effective until shortly after opening the instrument's cryoradiator cooler door on February 8, 2023 (or day 91 since launch). Unlike spectral bands on the VIS/NIR focal plane, the SWIR bands have shown a relatively large wavelength dependent decrease in their responses (or detector gains), up to 5% for M8 (1.24 μm) and M9 (1.38 μm). This feature is not present in N-20 SWIR bands. Compared to S-NPP, the N-21 VIIRS did not have large wavelength dependent degradation in its NIR bands over the same performance period. Because of large changes in SIWR responses, more frequent calibration look-up table (LUT) updates are necessary in order to maintain sensor on-orbit data quality. On the other hand, the TEB overall responses have been very stable, less than 1.0% for all bands, with most changes in the MWIR bands. Apart from the large data gap at mission beginning, there have been a few small data discontinuities or changes in spectral band responses, especially for the TEB, which are due to special operation or calibration events, such as MMOG, change of CFPA setting from 82K to 80K, and deep space pitch maneuver.

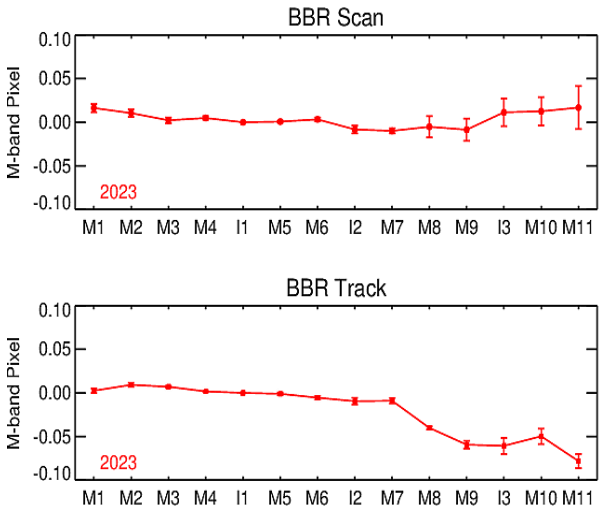

Fig. 5 RSB along-scan and along-track BBR derived from lunar observations.

Using regularly scheduled lunar observations, the sensor spatial performance can be evaluated via its band-to-band registration (BBR). Fig. 5 displays the results of N-21 VIIRS RSB BBR in both along scan and track directions. The BBR results in Fig. 5 are averaged over the first 3 lunar observations and referenced to M1, indicating excellent spatial performance with all BBR being within ±0.1 of the M-band pixel size.

As part of sensor radiometric performance assessments, the signal-to-noise ratios (SNR) are routinely computed for the RSB using detector responses to the sunlit SD. The computed SNR at different signal levels are fitted to a function to help derive the SNR at specified typical radiance levels. Similarly, the TEB noise equivalent temperature difference (NEdT) are measured at different temperatures during BB WUCD and at its nominal temperature (292.5 K) and results are scaled to their specified typical temperatures. Table 1 is a summary of VIIRS SNR design specifications for its VIS/NIR spectral bands (high gain only), and the N-21 pre-launch and on-orbit performance expressed using ratios of the measured to the specified SNR. As a result, ratios with values of larger than 1 correspond to better SNR

performance. Provided in Table 2 are the VIIRS TEB NEdT at specified typical scene temperatures), and the N-21 pre-launch and on-orbit performance via ratios of the measured to specified NEdT. In this case, ratios with values of less than 1 indicate better performance. Not included in Tables 1 and 2 are the SWIR bands and the low gains for the dual gain bands. Their SNR (or NEdT) performance also meet design requirements with margins.

Table 1 VIS/NIR SNR specification and performance (high gain only). PL: pre-launch; OO: on-orbit. Ratio = SNR (measured)/SNR (specified).

Band	I1	I2	M1	M2	M3	M4	M5	M6	M7
SNR Spec	119	150	352	380	416	362	242	199	215
PL Ratio	1.78	1.90	1.85	1.58	1.81	1.69	1.51	2.16	2.62
OO Ratio	1.66	1.89	1.84	1.55	1.71	1.61	1.51	2.08	2.48

Table 2 TEB NEdT specification and performance (high gain only). PL: pre-launch; OO: on-orbit. Ratio = NEdT (measured)/NEdT (specified).

Band	I4	I5	M12	M13	M14	M15	M16
NEdT Spec	2.5	1.5	0.40	0.11	0.09	0.07	0.07
PL Ratio	0.15	0.27	0.35	0.44	0.59	0.39	0.53
OO Ratio	0.16	0.24	0.39	0.38	0.46	0.31	0.35

Overall, the N-21 VIIRS performance is similar to N-20 and slightly better than S-NPP in terms of calibration stability. Although it is not presented in this paper, the N-21 DNB performance has also been very stable. Furthermore, the DNB stray light effect in the high gain stage is clearly smaller than that in S-NPP and N-20.

4. FUTURE IMPROVEMENTS

Current RSB calibration uses the SD BRDF and its screen transmittance function, and the SDSM screen transmittance function (all in relative terms) derived from measurements made during spacecraft yaw maneuvers. As more and more on-orbit calibration data become available, these parameters can be improved further. This improvement will likely help reduce small variations in the SD degradation trending shown in Fig. 2 as well as small and similar variations evident in the spectral response trending in Fig. 4 [10].

As mission continues, there will be additional regularly scheduled lunar observations, enabling an independent and more accurate monitoring of RSB calibration stability. Based on lessons from S-NPP and N-20, additional adjustments to the RSB calibration parameters derived from SD and SDSM will be made, including SD degradation at SWIR wavelengths as the on-board SDSM can only cover the wavelengths from 0.41 to 0.93 μm, and adjustments based on lunar trending. Remaining concerns of large changes in SWIR responses and the N-21 VIIRS calibration consistency with S-NPP and N-20 will be continuously examined and addressed accordingly.

5. ACKNOWLEDGEMENTS

We would like to acknowledge the contributions by other members of the NASA and NOAA VIIRS calibration teams.

6. REFERENCES

[1] Goldberg, M. D., H. Kilcoyne, H. Cikanek, and A. Mehta, "Joint Polar Satellite System: The United States next generation civilian polar-orbiting environmental satellite system", J. Geophys. Res.: Atmos., 118(24), 13,463–13,475, 2013.

[2] Lee, T., S. Miller, C. Schueler, and S. Miller, "NASA MODIS previews NPOESS VIIRS capabilities," Weather Forecasting, 21, 4, 649–655, 2006.

[3] Zhou, L., M. Divakarla, X. Liu, et al, "An Overview of the Science Performances and Calibration/Validation of Joint Polar Satellite System Operational Products," Remote Sens., 11, 698, 2019.

[4] Meyer, K., S. Platnick, R. Holz, et al., "Derivation of Shortwave Radiometric Adjustments for SNPP and NOAA-20 VIIRS for the NASA MODIS-VIIRS Continuity Cloud Products," Remote Sensing, 12 (24), 4096, 2020.

[5] Barnes, B. B., C. Hu, S. W. Bailey, et al., "Cross-calibration of MODIS and VIIRS long near infrared bands for ocean color science and applications," Remote Sensing of Environment, 260, 112439, 2021.

[6] Moon, M., X. Zhang, G. M. Henebry, et al., "Long-term continuity in land surface phenology measurements: A comparative assessment of the MODIS land cover dynamics and VIIRS land surface phenology products," Remote Sensing of Environment, 226, 74-92, 2019.

[7] Xiong, X., J. Butler, K. Chiang, et al., "VIIRS on-orbit calibration methodologies and performance," Journal of Geophysical Research, Vol. 119, Issue 9, 5065-5078, 2014.

[8] Cao, C., F. Deluccia, X. Xiong, et al., "Early On-Orbit Performance of the Visible Infrared Imaging Radiometer Suite Onboard the Suomi National Polar-Orbiting Partnership (S-NPP) Satellite," IEEE TGRS, Vol. 52, No. 2, 1142-1156, 2014.

[9] Oudrari, H., J. McIntire, X. Xiong, et al., "An Overall Assessment of JPSS-2 VIIRS Radiometric Performance Based on Pre-Launch Testing," Remote Sensing, 10, 1921, 2018.

[10] N. Lei and X. Xiong, "Determination of the NOAA-20 VIIRS screen transmittance functions with both the yaw maneuver and regular on-orbit calibration data", Applied Optics, vol 59, issue 10, pp. 2992-3001, 2020